Journal of Optoelectronics and Advanced Materials, Vol. 4, No. 3, September 2002, p. 513 - 521

STRUCTURAL PROPERTIES OF a-SiO_x LAYERS DEPOSITED BY REACTIVE SPUTTERING TECHNIQUE

N. Tomozeiu[a], J. J. van Hapert, E. E. van Faassen, W. Arnoldbik, A. M. Vredenberg, F. H. P. M. Habraken

Interface Physics, Debye Institute, Utrecht University, P.O. Box 80000, 3508-TA Utrecht, Netherlands,
[a]Faculty of Physics, Bucharest University, P.O. Box Mg-11, Bucharest, Romania

The SiO_x ($x<2$) layers deposited by sputtering around room temperature have been analyzed in terms of their compositional and structural properties. The layer thickness and composition have been determined using Rutherford backscattering (RBS). The deposition rate of silicon, oxygen and argon atoms is discussed as a function of x. Making use of the analysis of the Infrared Absorption spectra, we deduce that the structure of samples with $x<1.2$ is well described by the random bonding model (RBM). For samples with $x>1.2$, this agreement is not present and both the X-ray Photo-electron Spectroscopy and Electron Paramagnetic Resonance characterization techniques show a relatively large $Si(O_4)$ contribution in comparison to the predictions of the RBM model. The density of EPR active defects amounts to 10^{21} defects/cm^3.

(Received July 5, 2002; accepted July 22, 2002)

Keywords: a-SiO_x, Reactive sputtering, Fibers, XPS, EPR

1. Introduction

Amorphous silicon oxide (a-SiO) layers are very important in many electronic and optoelectronic applications. Gate insulator in MIS devices, passivation layers in microelectronics, optical transparent parts in optoelectronic devices are just a few examples of the wide use of a-SiO. The oxygen incorporation in the silicon matrix has a large influence on the physical properties of the obtained material. Although the non-crystalline silicon suboxides (a-SiO_x, with $x<2$) were studied for about 30 years [1] this research field is still very interesting from both a fundamental and a technological point of view. Thus, the results of the studies on a-SiO_x have proved in the last couple of years that this material is suitable for application in silicon based light-emitting devises [2].

It was also observed that the deposition technique influences the material properties. Various preparation methods were used to obtain thin a-SiO_x layers: Haga et al.[3] controlled the composition of the layers by changing the CO_2 and SiH_4 flow rate ratio in CVD depositions, Singh and Davis [4] have deposited by sputtering a SiO_2 target, Zacharias et al. [5] have obtained a-SiO_x:H by dc magnetron sputtering with water vapor as the oxygen source, Tsu et al [6] have prepared suboxide samples by plasma-enhanced chemical vapor deposition (PECVD) from $SiH_4/Ar/O_2/He$ gas mixture.

As other amorphous silicon compounds, a-SiO_x has the local structure based on a tetrahedral environment of the silicon. Two models which describe the global structure can be found in literature: i) the random bonding model (RBM) characterized by a continuous random network (CRN) of $Si(Si_{4-n}O_n)$ entities (a tetrahedral structure where one silicon atom is bonded with n oxygen atoms and 4-n silicon atoms)[1, 7-8], and ii) the random mixture model (RMM) where a separation in $Si(O_4)$ and

$Si(Si_4)$ phases is considered [9]. Many papers are devoted to a-SiO_x:H alloys in which the Si-H bond was used as a local probe for atomic structure. Thus, Tsu et al [6] have CRN modeled using chemically-induced shifts in the Si-H bond stretching frequency. Lucovsky [10] has shown that the CRN model is specific to the as deposited SiO_x:H films obtained in low-temperature plasma system. Annealing SiO_x films at T>800°C, the two phases model describes the structure of the same SiO_x films [11,12].

Changes in the local bonding from the as-deposited state to the annealed one at 900°C were studied by IR spectroscopy, especially the Si-O-Si bond-stretching mode absorption peak. Thus, prior to anneal, a-SiO_x:H films with different x values are characterized by a frequency of the Si-O-Si peak ranging between 1010 cm^{-1} and 1040 cm^{-1}, which is specific to homogeneous material [13]. By annealing at high temperature the same peak is moved to the 1080 cm^{-1} frequency region, characteristic of stoichiometric SiO_2. The SiH peaks from the IR spectrum disappear after annealing. Another important aspect is the photoluminescence of the as-deposited samples, which is not detectable for the annealed samples.

In many applications from microelectronics SiO_x films are formed at the interface between c-Si and SiO_2. Lucovsky [10] has shown that at a Si(111) – SiO_2 interface, which is not perfectly flat to have single Si dangling bond termination, there is a suboxide interfacial bonding arrangement related with the interface roughness. In ref [10] the author has proposed a model for this transition region where dangling bonds related to both the silicon and oxygen atoms are present.

In this paper we report about compositional and structural properties of thin SiO_x films deposited by reactive magnetron sputtering. A series of SiO_x samples ($0<x<2$) obtained by plasma sputtering of silicon from a silicon target in an Ar/O_2 atmosphere has been investigated. The Rutherford backscattering (RBS) technique is used to determine the composition of the layers. These results are related to the structural properties revealed by IR spectroscopy and X-ray Photoelectron Spectroscopy (XPS). The IR spectra are studied considering the structural entities built around the Si – O- Si bridge by n oxygen atoms and (6-n) silicon atoms that bond the bridge – edges. The interpretation of the Si 2p XPS spectra is based on tetrahedral structures as $Si(Si_4)$, $Si(Si_3O)$, $Si(Si_2O_2)$, $Si(SiO_3)$ and $Si(O_4)$. Both the IR and XPS investigations show that the SiO_x structure is RBM – like for x<1.2 and more RMM – like for x>1.2. In this paper are presented arguments for a structural phase changing of the SiO_x as deposited samples just by increasing the oxygen flow during deposition.

Dangling bond defects are investigated using Electron Paramagnetic Resonance (EPR) measurements. Their assignment to different structures supports the Infrared Absorption (IR) and X-ray Photo-electron Spectroscopy (XPS) results.

2. Experimental

Thin films of a-SiO_x were deposited using a 13.56 MHz reactive rf magnetron sputtering system. The power applied to the two plan parallel electrodes was 140 W. Silicon atoms were sputtered in a controlled oxidizing environment from a polycrystalline silicon target using Ar plasma. The deposition chamber was pumped down to a base pressure of less than $5\cdot10^{-7}$ mbar before the plasma gas (argon) was introduced. During deposition, the pressure was ~$5.6\cdot10^{-3}$ mbar and the substrate was at room temperature. The deposition system has a round target of diameter 100 mm and the distance between target and sample holder was 6 cm. Two types of substrates were used: i) c-Si (100) wafer for IR spectroscopy, XPS and ion beam analyses; ii) Corning glass for EPR measurements. Both substrates were covered on the same deposition run in order to guarantee a complete equivalence of the deposition conditions. The deposition time was calculated taking into account a layer thickness of about 200 nm for single layer samples. The deposition rate varies with the oxygen content, from 5.6 nm/min for a-Si to 12 nm/min for SiO_2. All samples were deposited using the same rf power and argon flow (80 sccm) while the oxygen flow vas varied between 0 and 0.8 sccm in steps of 0.1 sccm. No additional heating of the substrate was applied: during deposition the substrate temperature remained below 100°C.

The composition and thickness of the layers were determined by Rutherford backscattering spectrometry (RBS). The RBS measurements were done with a 2.4 MeV He^+ beam. The angle between the incoming beam and the sample surface was set at 65°. The detector was placed under an angle of θ=120° with the beam direction. The concentration and amount of the atoms of which a thin layer consists are obtained on an absolute scale with an accuracy of about 5%. However, no information is obtained about the chemical environment of the probed atoms.

The IR spectra of the samples were measured using a Digilab FTS-40 spectrometer equipped with a liquid-nitrogen cooled HgCdTe detector. The absorbance of the films was measured in the spectral range from 400 cm^{-1} to 4000 cm^{-1} with a resolution of 2 cm^{-1}.

X-ray Photoelectron Spectroscopy measurements have been performed using a Mg-K_α X-ray beam . The analysis of the energy of the emitted electrons was made using a CLAM-2 hemispherical sector analyzer with a pass energy of 20 eV. The resolution in binding energy is around 0.2 eV. The samples were transported through air from the deposition chamber to the XPS setup within 5 minutes.

EPR measurements were performed using a Bruker ESP 300 X-band spectrometer equipped with a rectangular cavity (TE102 mode, unloaded Q = 4000). The samples were cut to 2x20 mm^2 and loaded into a quartz tube (id = 4 mm) before being placed at the center of the cavity. The EPR spectra were measured at room temperature and the microwave power was 1.68 mW. The field modulation had a frequency of 100 kHz and an amplitude of 3370 G. The spectrometer time constant was 1.3 ms, the ADC conversion time was 5 ms and the receiver gain was 10^5. The microwave frequency was close to 9.4308 GHz. In addition, we carried out to saturation EPR experiments on two non-stratified samples with x=0.45 and 1.47 in order to probe the microwave saturation of the paramagnetic defects in the films. In this case, microwave power ranged between 0.4 mW and 164 mW. In this way we were able to distinguish different types of defects due to their different saturation behavior.

3. Results

3.1. Composition analysis

The RBS spectra have been analyzed using the RUMP code program which calculates the spectra for an assumed sample composition taking into account the effects of straggling, detector resolution, multiple scattering, etc [14]. Comparing the calculated spectra with the measured one, in successive approximation the absolute concentration depth profiles for elements from the sample are obtained. Table 1 shows the calculated values of the x parameter (i.e. SiO_x) when the oxygen flow was varied. In Fig. 1 are presented the deposition rate values of the atoms from the layer. The silicon atoms are deposited with a quasi-constant rate of ~$4.2 \cdot 10^{14}$ at./cm^2/sec while the variation of the oxygen content with the oxygen flow (in sccm) is described by:

$$O(at/cm^2/s) = 1.07 \times 10^{15} \cdot [O_2]^{1.46} \quad (1)$$

This empirical formula is specific to the deposition conditions presented in the previous section.

An interesting results shown in Fig 1. is the argon deposition rate. This has an averaged value of 3.8×10^{14} at./cm^2/sec, but depends slightly on the oxygen flow. A maximum was obtained for an oxygen flow of 0.6 sccm (x=1.22).

Table 1. Composition of the SiO_x thin layers via RBS measurements (± 5%).

$[O_2]$(sccm)	0.1	0.2	0.3	0.4	0.5	0.6	0.7	0.8
x	0.10	0.24	0.45	0.65	0.86	1.22	1.47	1.97

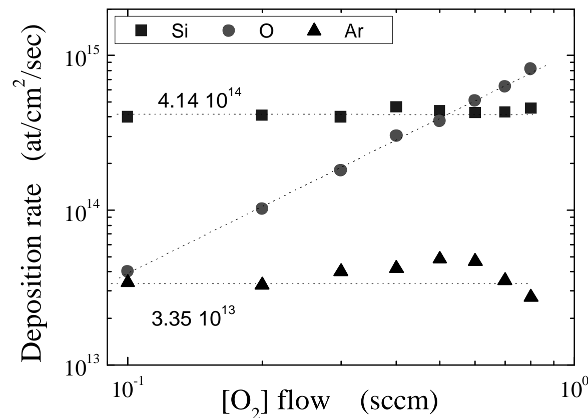

Fig. 1. The deposition rate (at/cm^2/sec) of silicon, oxygen and argon in SiO_x samples sputter deposited as a function of oxygen flow. Both the rf power and the argon flow have been the same during the series deposition.

3.2. Structural properties

The fingerprints of the Si-O-Si bonding group in an IR absorption spectrum are the vibrational rocking (350-500 cm^{-1}), bending (650-820 cm^{-1}) and stretching (940-1300 cm^{-1}) modes [15-18]. In this paper, the attention is focused on the stretching mode, which is the strongest spectral feature. Fig. 2 shows this region of the spectra for all samples. Their analysis revealed: a) a shift of the peak position towards higher wavenumbers when x increases; b) a shoulder in the region 1100-1250 cm^{-1} when $x > 1.2$. The shift of the peak position is due to the presence of the O-atoms neighboring Si-O-Si entities. Environments with different electro-negativity are created by adding more oxygen [15] and the bond strength is modified. Thus, the IR spectroscopy can be used to study the structural properties of the layer, but also as a technique to determine the oxygen concentration [5, 17].

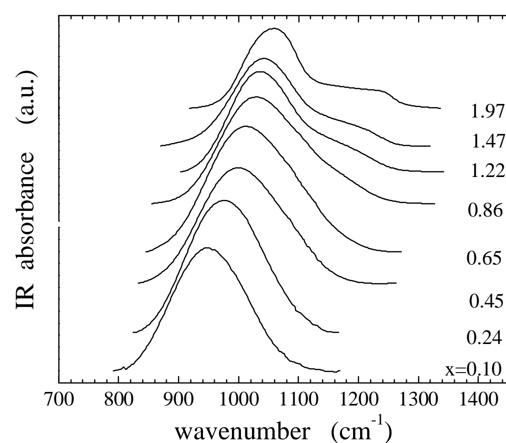

Fig. 2. Infrared absorption spectral region of the stretching vibration mode of the Si – O – Si bridge for various x values. When more oxygen atoms are bonded (x increases) the peak position is shifted to the right.

The shoulder appearing on the high wavenumber side of the principal peak is the fingerprint of the SiO_2 entity in the material structure. Its provenience is explained by Kirk [19] using a model of disorder-induced mechanical coupling between the active oxygen asymmetric stretch transverse-optic (TO) mode (in-phase motion of adjacent oxygen atoms) and the relatively optically inactive oxygen asymmetric stretch mode (out-of-phase motion of adjacent oxygen atoms). With these TO modes is paired a longitudinal-optic (LO) mode due to the interaction of the vibrational motion of the mode with the material's electromagnetic field through the electric charge on the vibrating atoms [19], which is only visible using non-perpendicular incident IR radiation, as is the case here. It appears that a long-range coupling of these vibrational modes of Si-O-Si bridge produces a more flat shoulder. We conceive the shoulder shape as an indicator for the presence of SiO_2 amount in the layers.

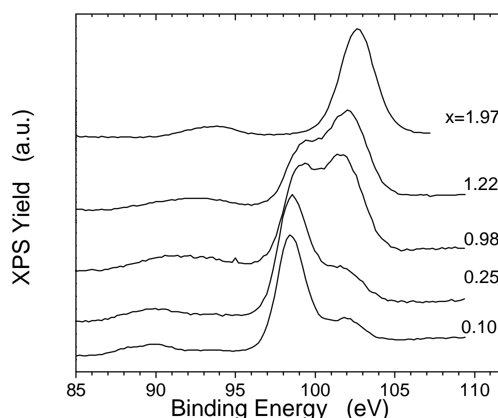

Fig. 3. Si 2p XPS spectra for SiO_x layers with different x values. A clear shift from $Si(Si_4)$ structure towards $Si(O_4)$ occurs when x increases.

Information about the presence of structural entities is also obtained from XPS measurements. Fig. 3 shows some representative spectra of the studied series. In the Si 2p spectra, increasing the oxygen content, an evolution towards higher binding energies of the main peak is observed. Such behavior has been reported before [20,21] and is explained by the charge transfer from Si to O atoms when Si-O bonds are formed. Considering a tetrahedral configuration around a silicon atom, the SiO_x structure is defined by structural entities as: pure Si, $Si(Si_3O)$, $Si(Si_2O_2)$, $Si(Si_3O)$ and SiO_2. As the oxygen content increases, there is an increase of the oxygen-richer components. For the sample $SiO_{1.97}$, the SiO_2 component represents almost all the signal. A five Gaussian functions fit of the Si 2p XPS spectrum revealed the contribution of each structural entity on the material structure. The results are reported in Fig. 4.

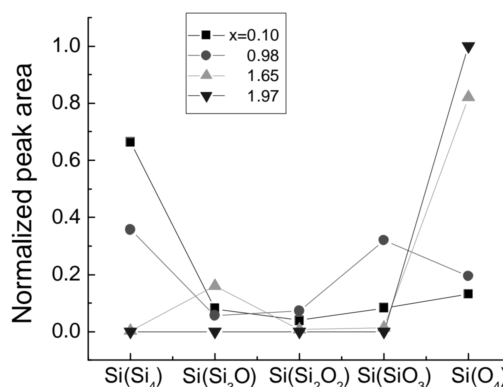

Fig. 4. The contribution of various structural entities to the structure of different SiO_x samples as derived from XPS.

The amorphous material structure is also characterized by defects, especially when the deposition process is based on particle bombardment. Information about defects' type and their density can be obtained with EPR measurements, where the paramagnetic defects are revealed. The first-derivative EPR spectra (not shown here) were the subject of Lorentzian functions fit in order to determine the values of the g factor – which defines the defect type. The spins density was calculated having as reference a MnO sample. Fig. 5 shows these results concerning both the g values and the spin density. According to the literature, a-Si dangling bond (DB) defects in the amorphous silicon structure are characterized by g=2.0057 and SiO_2 paramagnetic defects (E' centers) by g=2.0012 [22].

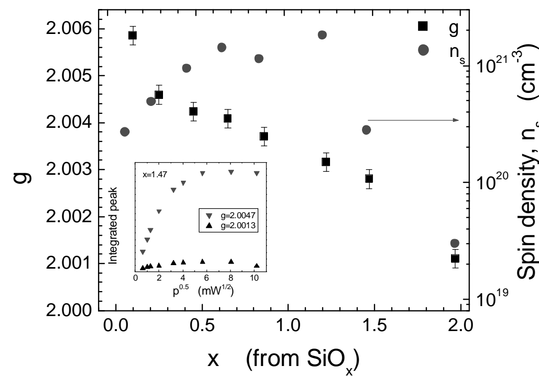

Fig. 5. Results of the EPR analyses in terms of the g-value (left hand scale) and the defect density (right hand scale).

4. Discussion

The samples' composition is a result of the physico-chemical processes that characterize the sputtering phenomena and the interactions between the particles from de gas phase with the substrate surface, under specific deposition conditions. Probably because the flow ratio between O_2 and Ar is smaller than 1/80, the oxygen flow variations seem not to influence the plasma conditions too much i.e. variation of the target voltage is within 5%. This is an explanation for the quasi-constant Si deposition rate shown in Fig. 1. Interesting is the shape of the Ar deposition rate versus the oxygen flow. As Fig. 1 shows, there is a turning point in the Ar concentration for oxygen flow at 0.6 sccm (x=1.2): for flows smaller than 0.6 the Ar concentration slightly increases with increasing O_2 flow and for larger flows it decreases significantly. In view of the observation that the plasma parameters remain constant we presume a constant Ar insertion in the layer. The variation in the Ar concentration is therefore assumed to find its origin in the structure of the grown layers. More explicitly: we assume that for the higher x values the material becomes increasingly more permeable for Ar to desorb from the layer. This suggests structural a change of SiO_x at x>1.2. The infrared spectra shown in Fig 2 agree with this idea. As can be seen the spectra for samples with x>1.2 "lose" a certain symmetry that is a characteristic of the random binding structure. Following a RBM calculation model proposed by Morimoto et al [23], where a random distribution of the Si-O-Si bonds has been considered, the presence probability of O-atoms nearby Si atoms can be calculated. Thus, the probability to have n O-atoms and 6-n Si-atoms neighboring the Si-O-Si bridge is:

$$P_n(x) = C_6^n P(Si)^{6-n} P(O)^n \qquad n = 0 \div 6 \tag{2}$$

where C_6^n gives the number of arrangements in which n sites are chosen in the 6 sites, P(Si) and P(O) being the probability of the presence of Si and O respectively.

For a given x value, the probability for Si-atom and O-atom to be bonded on the Si-O-Si bridge is:

$$P(Si) = 1 - \frac{x}{2} \quad \text{and} \quad P(O) = \frac{x}{2} \tag{3}$$

respectively, as defined in [23].

Using the relations (3) with (2), all the P_n (x) values can be calculated for each x value. Therefore, the contribution of a certain Si-O-Si related configuration can be theoretically predicted for each SiO_x structure.

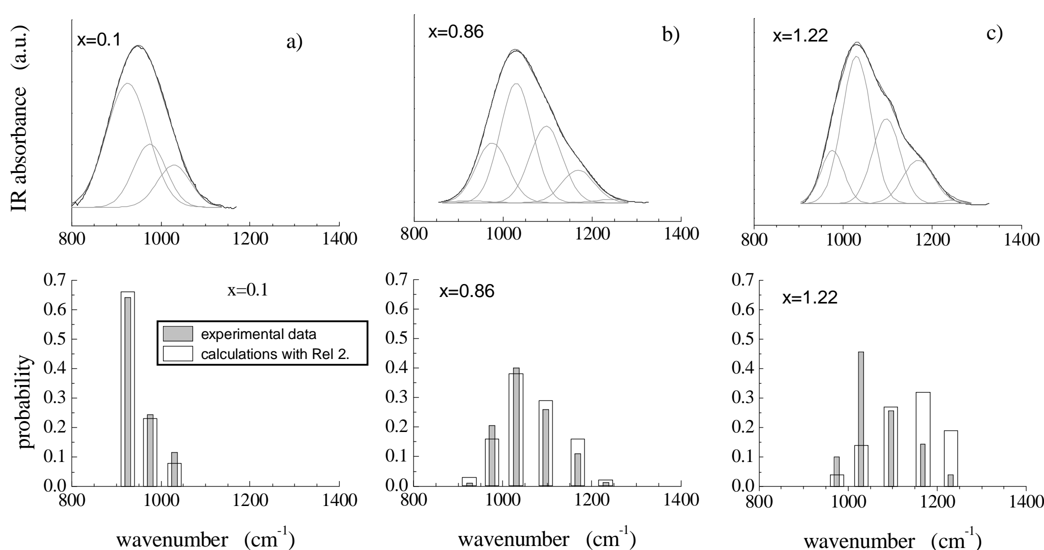

Fig. 6. Comparison of the deconvolution of IR spectra with the RBM structural model, for silicon - rich samples. The experimental data from the probabilities histogram represent the normalized peak area of each contribution.

On the other hand, the experimental absorption peak can be fitted with gaussians equidistant placed, each of them corresponding to a "n" value. The peak position for each gaussian was determined knowing the vibration frequency in a-Si (n=0) and in SiO_2 (n=6). The area of each gaussian contribution is proportional with the amount of related oscillators. Normalizing the area of each gaussian peak to the total peak area, the probability number predicted by theoretical calculation using Rel. (2) should be found, if the RBM describes the SiO_x structure. Such an example is presented in Fig. 6 where the fit results with six gaussians for samples with x=0.1 and x=0.86 are presented. For these samples, the comparison of the experimental data with the calculated probabilities is shown as a histogram in the same Fig 6. A good agreement of the experimental data fit with the theoretical model was found only for samples with x< 1.22. It has to be noted that the peak positions were found at the same wavenumber values within a 3% error. It was assumed on the theoretical calculations of probabilities that an oscillator with "n" oxygen atoms will have the same vibration frequency independently of the distribution of the "n" atom on six available sites.

Increasing the oxygen content, for x>1.2, the same model produces different results. First of all the fit quality is worse and the positions of the peaks are different from sample to sample. More than this, the analysis reveals a disagreement between the normalized area and the probabilities predicted (see Fig 6c).

Concluding, we suggest that for x<1.2, the material is characterized by a good homogeneity of its structure, and the RBM model can be applied in the structure studies. In the same time, the samples with x>1.2 are structured in such a way that the RBM model cannot be used to describe them. Many

papers [4-6, 9-10, 23-26] deal with oxygen-rich silicon suboxides with the RMM model. For SiO_x samples deposited by reactive sputtering, with x>1.2, the random mixing character has been shown using multilayered a-Si/SiO_2 structures [27]. Therefore x≈1.2 is the composition where the transition of the SiO_x from RBM-like structure to RMM-like occurs. The argon content (Fig. 1) has a maximum in this region and its decrease for larger values of x can be related to the larger oxygen rich and silicon rich structural clusters.

How do the XPS measurements reveal the two structural models? As the results reported in Fig 4 show, the samples with low x value are characterized by $Si(Si_4)$ and $Si(Si_3O)$ entities. Increasing the oxygen content, the contribution of these two components decrease and more $Si(SiO_3)$ is built-up. For instance, the structure of $SiO_{0.98}$ sample is formed from 35.7% $Si(Si_4)$, 5.6% $Si(Si_3O)$, 7.2% $Si(Si_2O_2)$, 32% $Si(SiO_3)$ and 19.4% $Si(O_4)$. Increasing the x values (x>1.22), the main contribution belongs to $Si(O_4)$. Tetrahedral entities as $Si(Si_4)$ and $Si(SiO_3)$ do hardly contribute. In these oxygen rich sub-oxides the $Si(Si_3O)$ represents the silicon-rich entity. The XPS data for the sample with x=1.97 show, in the error limit, only $Si(O_4)$ contributions. The results from Fig 4 reveal a very small contribution of the $Si(Si_2O_2)$ structural entities, independently on the x value. This is in good agreement with [25] where the authors have found that a structure based on Si^{3+}+Si^{+} species is more stable than a material constituted by Si^{2+} states.

A very important parameter determined by the structural characteristics is the density of defects. Energetically they are placed in the band gap and act as localized states in the electronic transport phenomena [28,29]. The neutral dangling bond density determined via EPR measurements amounts to about 10^{21} defects/cm^3 and, as Fig. 5 shows, varies with x. The characteristic energy of these defects, which will define their place in the band-gap, depends on the defect type. The EPR revealed defects are identified via the associated g factor. In literature are well defined so called a-Si dangling bonds centers (g=2.0057), specific to amorphous silicon material ($\cdot Si \equiv Si_3$) [30], and the E' centers (g=2.0012), which is specific to silicon dioxide glasses ($\cdot Si \equiv O_3$) [22]. In between these limits the g factor, which characterize the SiO_x layers studied in this paper, varies with x as the Fig 5 shows. When the oxygen content in the layer increases, the g value decreases. This should be related with more oxygen neighboring of the defect site. Molecular orbital calculations have confirmed a monotonic decrease of the g values with increasing the x value, using various structural entities [31]. We could not check this model on our g data presented in Fig 5 because of the lack of highly resolved EPR spectra.

In order to check the contribution of different defect types at a broad EPR spectrum, EPR measurements at various microwave power have been performed. In this way the saturable defects have been revealed. Some of the results are already reported [27]. The silicon - rich samples contain a single non-saturable type of defect assigned to a-Si dangling bonds (DB) with g values ranging between 2.0057 and 2.004. This variations could be related to the different values of Si – Si bond length and Si – O – Si bond angle from the SiO_x structure and to an environment with various electronegativities. The samples with high x values contain two defects: the first one is nonsaturable and assigned to Si DB, whereas the second is saturable and attributed to the E' found in SiO_2 domains (see the insert from the Fig 5. These results support the RBM for silicon – rich SiO_x and RMM for oxygen – rich structures.

5. Conclusions

The elemental composition and thickness of the SiO_x layers, as revealed by RBS show that the deposition rate of Si atoms is constant during RF-magnetron sputtering. The O and Ar deposition rate do depend on the oxygen partial pressure in the gas phase.

It has been shown that the RBM model describes the SiO_x structure for x<1.2. The IR analysis support the model that a randomly distribution of the Si – Si and Si – O bonds characterizes these samples. The EPR results show a defect density in the range of 10^{20} – 10^{21} defects/cm^3 having a broad maximum for 0.5 < x < 1.2.

The IR spectra of the samples with x>1.2 have proved that the RBM model is not applicable to describe the material structure at high oxygen concentrations. In agreement with that, the XPS spectra

also favor the RMM model. EPR defect saturation measurements have shown two types of defects: one silicon dangling bond related and the second one E' centers – specific to SiO_2.

As a result of this study it appears that two different SiO_x structures can be obtained in the same deposition process if the composition of the layers varies from silicon–rich to oxygen–rich. It has been shown that $x \approx 1.2$ is a transition composition from RBM to RMM SiO_x structure.

References

[1] H. R. Philipp, J. Non-Cryst. Solids **8-10**, 627 (1972).
[2] A. Stick, M. Markmann, K. Brunner, G. Abstreiter, E. Muller – Materials Science and Engineering **B89**, 274 (2002).
[3] K. Haga, H. Miura, M. Kumano, H. Watanabe, J. Non- Cryst. Solids **115**, 126 (1989).
[4] A. Singh, E. A. Davis, J. Non-Cryst. Solids **122**, 223 (1990).
[5] M. Zacharias, T. Drusedau, A. Panckow, H. Freistedt, B. Garke, J. Non- Cryst. Solids **169**, 29 (1994).
[6] D. V. Tsu, G. Lucovsky, R. N. Davidson, Phys. Rev. **B40** 1795 (1989).
[7] H. R. Philipp, J. Phys. Chem. Solids **32** 1935 (1971).
[8] H. R. Philipp, J. of the Electrochem.Soc.,**120**(2), 295 (1973).
[9] K. Haga, H. Watanabe, J. Non-Cryst. Solids **195**, 72 (1996).
[10] G. Lucovsky, J. Non-Cryst. Solids **227-230**, 1 (1998).
[11] M. Hamasaki, T. Adachi, S. Wakayama, M. Kikuchi, J. Appl. Phys. 49, 3987 (1978).
[12] J. Ni, E. Arnold, Appl. Phys. Lett. **39**, 554 (1981).
[13] S. S. Chao, J. E. Tyler, Y. Takagi, P. G. Pai, G. Lucovsky, S.Y. Lin, C.K. Wong, M.J. Martini, J. Vac. Sci. Thech. **A4**, 1574 (1986).
[14] L. R. Doolittle, Nucl. Instr. & Methodes **B9**, 344 (1985).
[15] G. Lucovsky, J. Yang, S. S. Chao, J. E. Tyler, W. Czubatyi, Phys. Rev. **B28**, 6, 3225 (1983)
[16] A. Sight, E. A. Davis, J. Non-Cryst Solids, 122, 223 (1990).
[17] P. G. Pai, S. S. Chao, Y. Takagi, G. Lucovsky, J. Vac. Sci. Technol. **A 4 (3)**, 689 (1986).
[18] T. Hirata, J. Phys. Chem. Solids **58**, 1497 (1997).
[19] C. T. Kirk, Phys. Rev. **B38**, 2, 1255 (1988).
[20] F. J. Himpsel, F. R. McFeely, A. Taleb-Ibrahimi, J. A. Yarmoff, G. Hollinger, Phys. Rev. **B38,** 9, 6084 (1988).
[21] R. Alfonsetti, L. Lozzi, M. Passacantando, P. Picozzi, S. Santucci, Appl. Surf. Sci. **70/71** 222 (1993).
[22] W. L. Warren, E. H. Poindexter, M. Offenberg, W. Muller-Warmuth, J. Electrochem. Soc. **139** 872 (1992).
[23] A. Morimoto, H. Nariyama, T. Shimizu, Jap. J. of Applied Phys. **26**, 1, 22 (1987).
[24] F. Stolze, M. Zacharias, S. Schippel, B. Garke, Solid State Communications **87**, 9, 805 (1993).
[25] A. Barranco, J.A. Mejias, J. P Espinos, A. Caballero, A. R. Gonzalez-Elipe, F. Yubero, J. Vac. Sci. Technol. A 19 (1), 136 (2001).
[26] D. M. Wolfe, G. Lucovski – J. Non Cryst. Sol. 266, 1009 (2000).
[27] N. Tomozeiu, E. E. van Faassen, W. M. Arnoldbik, A. M. Vredenberg, F. H. P. M. Habraken, Thin Solid Films (in press).
[28] M. H. Cohen, H. Fritzsche, S. R. Ovshinsky, Phys. Rev. Letters **22**, 1065 (1969).
[29] J. J. van Hapert, PhD Thesis, Utrecht University, 2002.
[30] P. Thomas, M. Brodski, D. Kaplan, D. Lepine, Phys. Rev. **B18**, (1978) 3059.
[31] T. Inokuma, L. He, Y. Kurata, S. Hasegawa, Journal of the Electrochemical Society **142**, 2346 (1995).